ARTICLE

Hydrogen Bond Networks in Graphene Oxide Composite Paper: Structure and Mechanical Properties

Nikhil V. Medhekar,[†] Ashwin Ramasubramaniam,[‡] Rodney S. Ruoff,[¶] and Vivek B. Shenoy[†,*]

[†]Division of Engineering, Brown University, Providence, Rhode Island 02912, [‡]Department of Mechanical and Industrial Engineering, University of Massachusetts, Amherst, Massachusetts 01003, and [¶]Department of Mechanical Engineering, University of Texas, Austin, Texas 78712

ABSTRACT A multilayered composite structure formed by a random stacking of graphene oxide (GO) platelets is an attractive candidate for novel applications in nanoelectromechanical systems and paper-like composites. We employ molecular dynamics simulations with reactive force fields to elucidate the structural and mechanical properties of GO paper-like materials. We find that the large-scale properties of these composites are controlled by hydrogen bond networks that involve functional groups on individual GO platelets and water molecules within the interlayer cavities. Water content controls both the extent and collective strength of these interlayer hydrogen bond networks, thereby affecting the interlayer spacing and elastic moduli of the composite. Additionally, the chemical composition of the individual GO platelets also plays a critical role in establishing the mechanical properties of the composite—a higher density of functional groups leads to increased hydrogen bonding and a corresponding increase in stiffness. Our studies suggest the possibility of tuning the properties of GO composites by altering the density of functional groups on individual platelets, the water content, and possibly the functional groups participating in hydrogen bonding with interlayer water molecules.

KEYWORDS: graphene oxide · graphene oxide composite paper · structure · mechanical properties · molecular dynamics simulations

In recent years, graphene—a single layer of carbon atoms arranged in a honeycomb lattice structure[1]—has emerged as a promising material for novel applications in nanoelectronic and spintronic devices,[2,3] sensing,[4] and energy storage technologies.[5] Among several techniques used to produce graphene-based sheets, the chemical treatment of functionalized graphitic compounds such as graphene oxide (GO) is an efficient and versatile option.[6] Apart from being a precursor for graphene, GO itself can be useful in flexible electronics,[7] in battery electrodes,[8] and as a paper-like composite material.[9−12]

Because of its outstanding mechanical properties, GO has attracted significant interest as a building block for novel applications in composites,[9,10] transparent paper-like materials,[11,12] mechanical actuators,[13] nanorobots,[14] and nanoelectromechanical systems.[14] GO composites are typically fabricated from colloidal suspensions of GO sheets in water.[15,16] X-ray diffraction measurements suggest that the composite material has a layered structure with a mean interlayer distance in the range of 6−11 Å.[11,17,18] Since GO is hydrophilic, interlamellar water molecules are always present in interlayer voids even after prolonged drying.[11] Nevertheless, these materials display remarkable mechanical properties with tensile moduli being in the range of 6−42 GPa and fracture strengths of 100−132 MPa.[11,12]

Recent experiments have shown that the large-scale structural, mechanical, and electronic properties of GO composites are strongly influenced by atmospheric humidity.[11,17−19] For instance, when the relative humidity is increased from a negligible level to 100%, the composite structure swells in volume by more than 70% due to the absorption of water[17,18] and the tensile modulus decreases substantially.[11] Although a significant amount of work has focused on characterizing isolated GO layers,[20−23] the atomic-level origins of the mechanical properties of GO paper—which is composed of stacked GO platelets and interlamellar water molecules—remain to be addressed. The key to understanding the mechanical properties of GO paper lies in examining the *collective* behavior of stacked platelets along with the interlayer adhesive (water molecules).

In this article, we elucidate the atomic-level structure and mechanical properties of GO paper based on molecular dynamics simulations using the ReaxFF reactive force field.[24] We find that the individual GO platelets are interlinked *via* a non-uniform network of hydrogen bonds mediated by oxygen-containing functional groups and water molecules. A quantitative analysis of the formation of hydrogen bond networks further shows that they play a central role in

*Address correspondence to vivek_shenoy@brown.edu.

Received for review December 31, 2009 and accepted March 5, 2010.

Published online April 9, 2010.
10.1021/nn901934u

determining the overall morphology and mechanical properties of GO paper materials. Our predicted structural and mechanical properties are in good agreement with experimental observations.

RESULTS AND DISCUSSION

To obtain the atomic-level structure of hydrated GO at equilibrium, we constructed a periodic supercell containing four 3.4 nm × 3.0 nm GO platelets. We chose two chemical compositions of individual GO layers: $C_{10}O_1(OH)_1$ and $C_{10}O_2(OH)_2$ (*i.e.*, one and two epoxy and hydroxyl groups per 10 carbon atoms, distributed randomly on either side of the graphene basal plane). While a significant control over the overall composition and the distribution of oxygen-containing functional groups can be achieved during the preparation of GO, the two cases we have chosen represent a typical and likely outcome of the oxidation process during the preparation of GO platelets.[25] Using this supercell, we performed extensive molecular dynamics simulations using the reactive force field ReaxFF in order to understand the atomic-level structure and the origins of mechanical properties of GO composites.[26,27] See Methods for a detailed description of the supercell geometry and the computational procedure to obtain the equilibrium structure and mechanical properties.

To study the influence of interlamellar water coverage on the structure of multilayered GO, we first systematically varied the water fraction from 1 to 26 wt %. Figure 1 shows the atomic structure of multilayer GO with a chemical composition of $C_{10}O_1(OH)_1$ obtained for two different hydration levels; we readily note several qualitative differences between the structures at different hydration levels. When the water content is negligible (Figure 1a), the composite displays a more uniform, tightly bound structure with a small interlayer distance of 5.1 Å. In contrast, GO at 26 wt % water content displays a significantly nonuniform structure—the individual layers are separated by clusters of water molecules, resulting in a large interlayer distance of 9.0 Å. This observation of the agglomeration of the water molecules is consistent with the neutron scattering measurements at high humidity levels that report a significant nonlocal motion associated with the agglomerated water molecules in the clusters.[17] A more quantitative analysis of our data shows that the interlayer distance for hydrated GO paper varies linearly with water content, as shown in Figure 2. When the water content is increased from negligible levels to 26 wt %, the interlayer distance increases from 5.1 to 9.0 Å; the volume of GO swells by 76%. The variation of interlayer distance is *independent* of the chemical composition of the GO layers and depends only on the water content. We find that these observations are in excellent agreement with experimental measurements, which report typical interlayer distances in the range of 6.0 to 11.0 Å, depending on the relative humidity.[17,18]

The humidity-dependent properties of the GO paper can be understood by examining the hydrogen bond (H-bond) network between the interlayer water molecules and the epoxy and hydroxyl functional groups on individual GO platelets. A hydrated GO composite typically displays various configurations of the O···H bonds, as shown schematically in Figure 3a. While the donor hydrogen and the acceptor oxygen at-

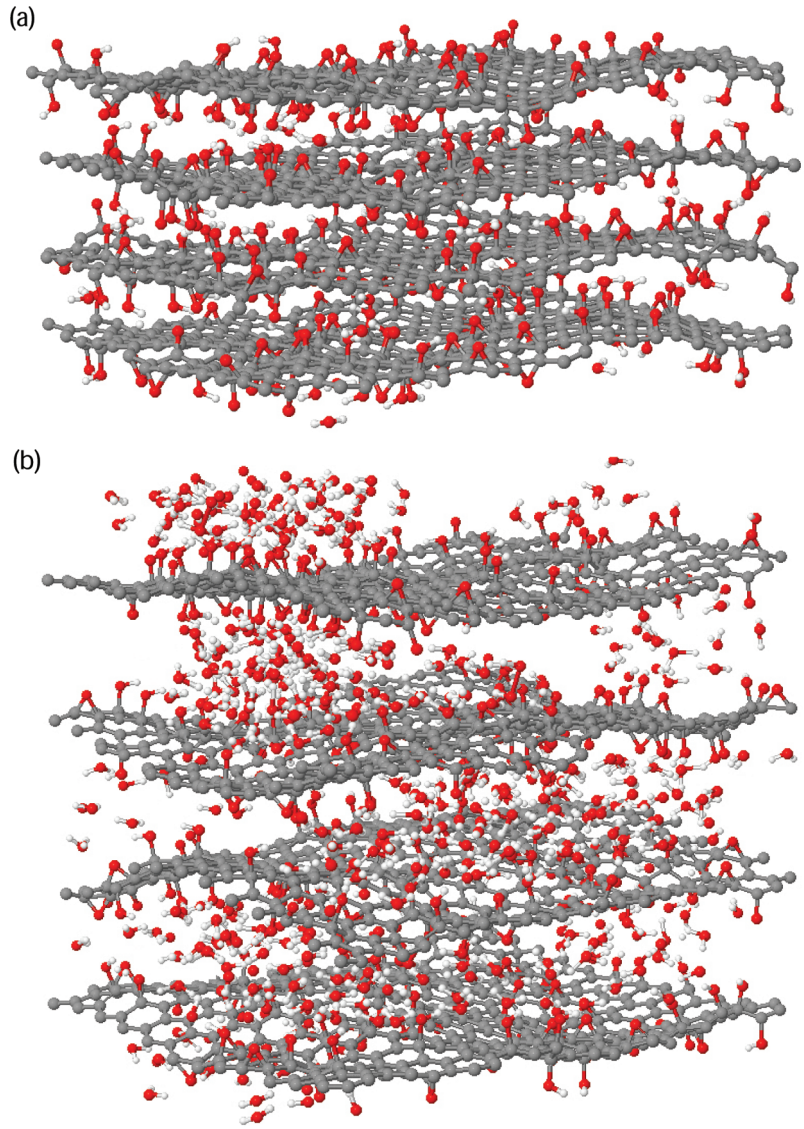

Figure 1. Atomic structure of hydrated multilayer GO at 300 K containing (a) 0.9 and (b) 25.8 wt % of water. The individual GO layers are 3.4 nm × 3.0 nm and have a chemical composition of $C_{10}O_1(OH)_1$. The average interlayer distances are (a) 5.1 Å and (b) 9.0 Å. Carbon, oxygen, and hydrogen atoms are represented by gray, red, and white spheres, respectively.

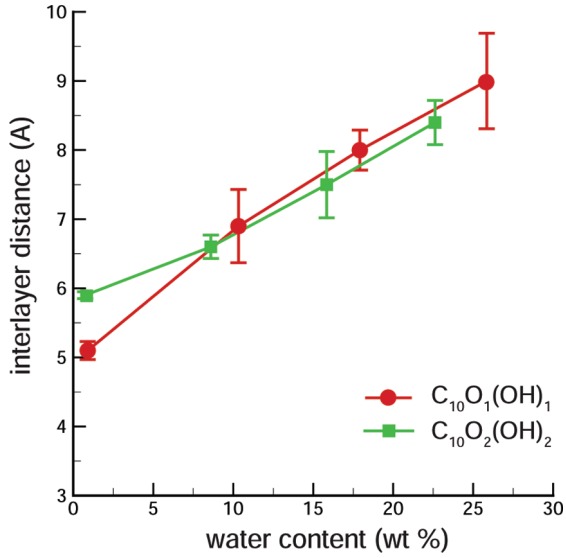

Figure 2. Variation of interlayer distance as a function of water content for GO with a chemical composition of $C_{10}O_1(OH)_1$ (red) and $C_{10}O_2(OH)_2$ (green).

oms are, in general, covalently bonded to different functional groups, the strength of the O···H bonds shown in Figure 3a is similar. By computing the energy of interaction between two water molecules connected by a single H-bond (see Figure 3b), we determined the optimal O···H bond distance to be 2.55 Å with a bond strength of 320 meV. These values are in agreement with earlier reported estimates for a typical O···H bond,[28] which indicates that the ReaxFF potential is expected to predict reasonable structural and mechanical properties for materials dominated by H-bonds.

Next, we analyze in detail the nature and extent of H-bonding within the equilibrated GO structures. Figure 4a shows the variation of the total number of H-bonds as a function of water content for chemical compositions $C_{10}O_1(OH)_1$ and $C_{10}O_2(OH)_2$. For both structures, the total number of H-bonds increases almost linearly with water content. As expected, the structure with a chemical composition of $C_{10}O_2(OH)_2$ has more H-bonds than $C_{10}O_1(OH)_1$ at all hydration levels, due to the presence of twice as many epoxy and hydroxyl functional groups that can participate in the formation of H-bonds. The H-bonds in the composite structures may be further subdivided into the following categories: (1) H-bonds between functional groups attached to the same graphene sheet (intralayer), (2) H-bonds between the functional groups attached to adjacent graphene sheets (interlayer), and (3) H-bonds involving water molecules. These three categories are displayed separately for the two GO structures in Figure 4b. At low hydration levels, the H-bond network is dominated by the bonds between the hydroxyl and epoxy functional groups (intra- and interlayer). Consequently, the composite attains a compact structure with small interlayer distances (5−6 Å), as seen in Figure 2. At high hydration levels, we see that the H-bond network is dominated by bonds with water molecules. The GO platelets are now well-separated and do not interact directly with each other; instead, their interaction is mediated by a network of H-bonded water molecules.

We further classified the H-bonds involving water molecules into bonds between a water molecule and a functional group and the bonds between any two water molecules, as shown in Figure 5. In the case of GO with a chemical composition of $C_{10}O_1(OH)_1$ (Figure 5a), water molecules form H-bonds primarily with epoxy and hydroxyl functional groups at low hydration levels. Moreover, due to the low density of functional groups, water molecules form, on average, either one or zero H-bonds. With increasing water content, we have more than one H-bond per water molecule, as seen from Figure 5a. In other words, some water molecules are bonded with more than one water molecule or functional group, thereby forming a H-bond network. At the same time, accumulation of water molecules between the GO platelets leads to a reduced number of interlayer H-bonds, as seen from Figure 4b), and results in a larger interlayer spacing. As the water content increases beyond 15 wt %, we see that the H-bond network is dominated by water−water H-bonds. The GO platelets are only connected indirectly through chains of water molecules, as seen in Figure 2. In the case of the $C_{10}O_2(OH)_2$, the formation of H-bond networks is essentially similar with a few minor differences. As seen from Figure 5b, for low water content, the

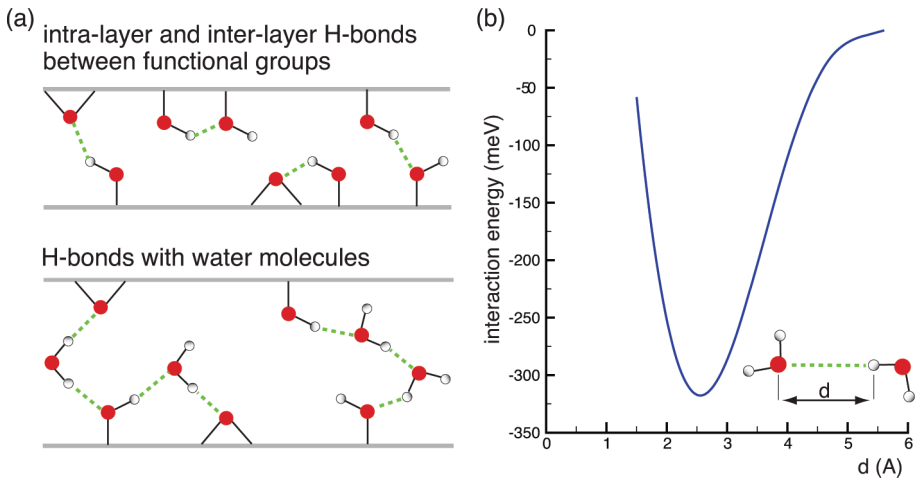

Figure 3. (a) Schematic showing various configurations of hydrogen bonds in the hydrated GO composite. The horizontal gray lines denote the graphene sheet, while oxygen and hydrogen atoms are shown as red and white spheres, respectively. (b) Variation of the O···H bond energy (computed as the interaction energy between two water molecules) as a function of bond distance *d*. The optimum O···H bond distance is 2.55 Å, and the bond strength is 320 meV.

number of hydrogen bonds per water molecule (1.2) is larger than that for $C_{10}O_1(OH)_1$; a larger density of functional groups in $C_{10}O_2(OH)_2$ implies that some water molecules can form more than one H-bond with the functional groups. Again, as in the case of $C_{10}O_1(OH)_1$, an extensive H-bond network is developed at high hydration levels (Figure 5b), resulting in structures with large interlayer distances.

Finally, we investigate the influence of H-bond networks on the mechanical properties of the multilayered GO composite structure. In the experiments characterizing the mechanical properties of these structures,[11] the lateral dimensions of test specimens (~few centimeters) are much larger than the mean lateral size of GO platelets (~1 μm). In the absence of any interlayer covalent bonding, the platelets interact with each other only through H-bond networks. Therefore, the overall mechanical behavior of the composite is expected to be governed by the strength of H-bond networks. We have estimated the strength of these networks by computing the elastic modulus in the direction normal to the sheets using atomic displacement correlation functions (see Methods). The elastic modulus is strongly influenced by water content—it drops by more than 50% beyond 20 wt % water content. This behavior may be understood as follows. When the structure is relatively dry, any macroscopic deformation essentially translates to stretching of interlayer H-bonds. However, when there are significant amounts of water present in the interlayer space, H-bond stretching is not the sole mechanism for accommodating deformations. Since the water molecules possess rotational degrees of freedom, they can also reorient themselves (thus breaking and making new H-bonds) in response to the external load. The reorientation of water molecules thus minimizes the strain in H-bonds. We also see from Table 1 that the $C_{10}O_2(OH)_2$ structure consistently exhibits larger values of the modulus than the $C_{10}O_1(OH)_1$ structure at comparable levels of water content. This composition-dependent behavior is readily understood by noting that the $C_{10}O_2(OH)_2$ structure has more hydroxyl and epoxy groups than the $C_{10}O_1(OH)_1$ structure, which then allows for the formation of more H-bonds between neighboring layers, thereby strengthening interlayer adhesion.

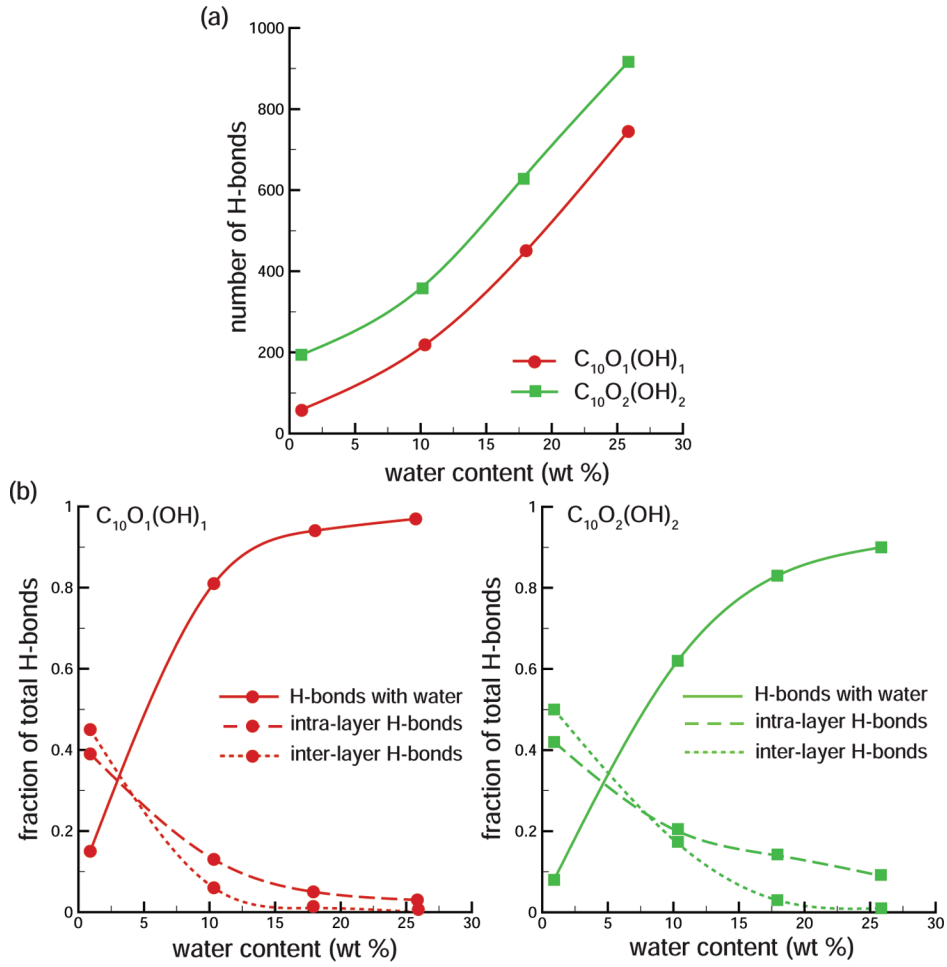

Figure 4. Statistics for O···H bonds in hydrated GO composites with chemical compositions of $C_{10}O_1(OH)_1$ and $C_{10}O_2(OH)_2$ as a function of water content. (a) Total number of O···H bonds, and (b) the fraction of total O···H bonds contributed by the different configurations shown in Figure 3a: intralayer and interlayer O···H bonds between the functional groups, and O···H bonds involving water molecules.

We find that the computed elastic moduli, which are completely controlled by interlayer H-bond networks, are within the range of experimental measurements (6−42 GPa[11,12]). Moreover, the hydration-dependent behavior of the computed elastic moduli shown in Table 1 is also in qualitative agreement with experiments, which report a decrease in elastic modulus and tensile strength of GO paper subjected to increasing humidity levels.[11] However, two important differences between the computation of elastic constants and the experimental measurements should be noted. Our computational sample consists of stacked GO sheets of infinite extent and essentially represents a simplified model of the realistic test specimens. On the other hand, the realistic test specimens of the GO paper used in experiments have lateral dimensions of a few centimeters and consist of randomly stacked micrometer-sized GO platelets. Moreover, the test

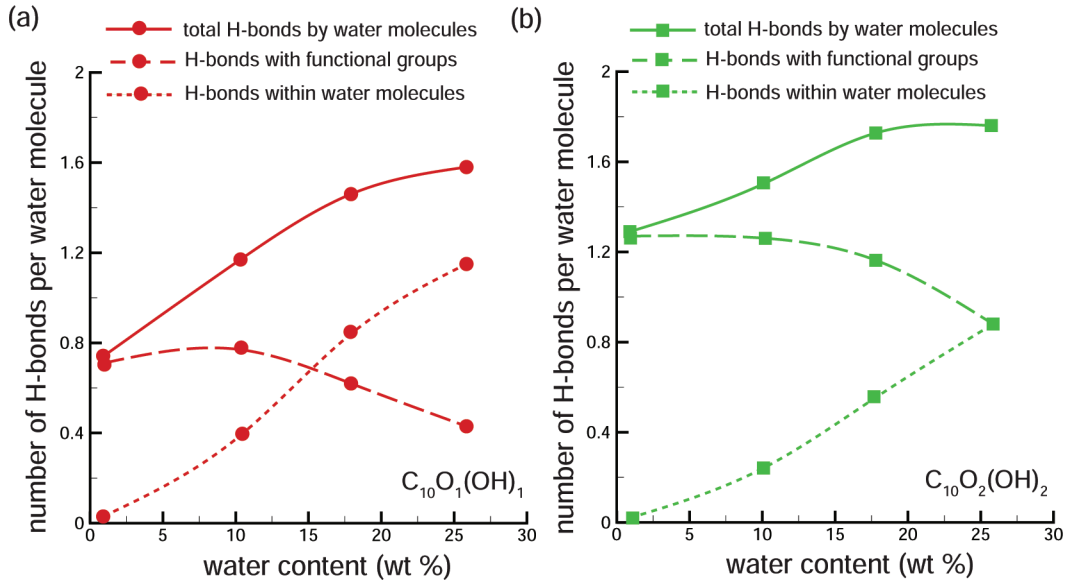

Figure 5. Variation of the number of hydrogen bonds per water molecule as a function of the water content for GO with chemical compositions of (a) $C_{10}O_1(OH)_1$ and (b) $C_{10}O_2(OH)_2$. The hydrogen bonds formed by water molecules are further classified into the bonds between a water molecule and a functional group and the bonds between any two water molecules.

specimens are also characterized by the presence of micrometer-sized voids separating the platelets.[11] Unfortunately, these realistic length-scales are prohibitively large for fully atomically resolved simulations.

The second noteworthy difference with the experimental measurements is that the realistic test specimens always contain platelets that are crumpled, folded, and entangled with each other. Consequently, the direction of load transfer among the neighboring GO platelets can be along or perpendicular to the macroscopic deformation depending on their local orientations. Nevertheless, in the absence of interlayer covalent bonding, the overall strength can only be attributed to the stretching of individual hydrogen bonds between adjacent platelets. In our model geometry, the elastic modulus that is completely governed by the stretching H-bond interactions is the tensile modulus in the direction normal to the GO sheets. We find that the computed shear modulus is much lower than the normal modulus, as the epoxy and hydroxyl groups and water molecules can reorient with relative ease when the composite structure is subjected to shear deformation in the direction along the sheets in comparison with the deformation in the direction normal to the sheets.

Despite the differences between the model geometry and the realistic test specimens, our model clearly establishes the role of H-bond networks in determining the overall structural properties as seen earlier from the variation of interlayer distance with hydration levels. Our approach also captures the key deformation mechanism involving the stretching of H-bonds. While the elastic moduli computed for chemical compositions $C_{10}O_1(OH)_1$ and $C_{10}O_2(OH)_2$ of the model geometry are lower than 20 GPa, they nevertheless provide the correct order of magnitude estimates for the measured elastic moduli (6−42 GPa). In more realistic morphologies, the interactions between entangled and folded platelets can add to the H-bond-induced strengthening effects and may perhaps explain the higher moduli (larger than 30 GPa) measured in some test specimens.

TABLE 1. Elastic Modulus (GPa) Controlled by the Interlamellar Hydrogen Bond Networks in the GO Composite Structures as a Function of Water Content (wt %)[a]

$C_{10}O_1(OH)_1$		$C_{10}O_2(OH)_2$	
water content	modulus	water content	modulus
0.9	6.3	0.7	14.4
10.3	4.8	8.6	18.6
17.9	3.9	15.8	9.7
25.6	3.6	22.6	5.0

[a]The modulus is computed at 300 K using the atomic displacement correlation functions (see Methods).

CONCLUSIONS

In conclusion, we have performed systematic molecular dynamics simulations to elucidate the structural and mechanical properties of GO paper-like samples. We have shown that the properties of these composites are essentially controlled by H-bond networks involving both functional groups attached to GO platelets as well as water molecules within the interlayer cavities. We find that moisture content controls both the extent as well as the collective strength of interlayer H-bond networks, which is in turn manifested in the overall macroscopic response of these materials. Dry GO sheets are structurally more compact and more stiff than moist sheets. Furthermore, the stiffness of these paper-like materials increases with the density of func-

tional groups due to greater interlayer adhesion. Our studies suggest the possibility of tuning both the structural and mechanical properties of GO papers by varying the extent of functionalization of individual platelets as well as the overall water content in the material. Finally, since the mechanical behavior of this composite is controlled largely by H-bond networks (O···H in the present study), one may also envision tuning the strength of the GO paper by functionalizing the individual platelets with other atomic species/functional groups that are capable of participating in H-bonding with water.

METHODS

The periodic supercell used in molecular dynamics simulations consists of four 3.4 nm × 3.0 nm GO platelets separated initially by a distance of 7 Å. Epoxy and hydroxyl functional groups were randomly distributed on the two sides of the graphene sheets, while water molecules were randomly dispersed in interlayer cavities. The molecular dynamics simulations were carried out using the ReaxFF reactive force field as implemented in the LAMMPS simulation package.[26,27] This force field has been shown to provide an accurate description of hydrocarbons and water.[27] ReaxFF also allows for an explicit consideration of long-range and nonbonded interactions such as van der Waals, Coulombic, and hydrogen bond interactions, making it particularly suitable for our study of multilayer GO. The structure was first equilibrated using an NPT ensemble with the Nosé−Hoover thermostat[29] and barostat[30] for temperature and pressure control, respectively, at a time step of 0.025 fs. The supercell was first gradually heated from 10 to 1000 K over a time span of 625 fs, then annealed at 1000 K for 625 fs, and subsequently quenched to 300 K over a time span of 625 fs. Finally, the supercell was further annealed at 300 K and zero pressure for the duration of 4.25 ps to ensure complete equilibration of the structure.

After this equilibration phase, we switched to an NVT ensemble at 300 K in order to estimate the mechanical strength of GO composites due to the interlamellar hydrogen bond networks. The atomic displacement data were recorded at every 50 time steps to compute the displacement correlation functions. The elastic constant of the structure determined by the hydrogen bond networks can then be readily obtained in the long wavelength approximations from the correlation function in the direction normal to the sheets.[31,32] Since this method of computing elastic constants relies solely on atomic displacements rather than local strain or stress measures, it is particularly appropriate for our study of nonhomogeneous GO structures.

Acknowledgment. N.V.M. and V.B.S. gratefully acknowledge research support from the NSF and NRI through the Brown University MRSEC program and the NSF through Grants CMMI-0825771 and CMMI-0855853. The computational support for this work was provided by Grant TG-DMR090098 from the TeraGrid Advanced Support Program and the Center for Computation and Visualization at Brown University. RSR was supported by the U.S. Department of Energy, Office of Basic Energy Sciences, Division of Materials Sciences and Engineering under Award ER46657.

REFERENCES AND NOTES

1. Geim, A. K.; Novoselov, K. S. The Rise of Graphene. *Nat. Mater.* **2007**, *6*, 183–191.
2. Berger, C.; Song, Z. M.; Li, X. B.; Wu, X. S.; Brown, N.; Naud, C.; Mayou, D.; Li, T. B.; Hass, J.; Marchenkov, A. N.; Conrad, E. H.; First, P. N.; de Heer, W. A. Electronic Confinement and Coherence in Patterned Epitaxial Graphene. *Science* **2006**, *312*, 1191–1196.
3. Tombros, N.; Jozsa, C.; Popinciuc, M.; Jonkman, H. T.; van Wees, B. J. Electronic Spin Transport and Spin Precession in Single Graphene Layers at Room Temperature. *Nature* **2007**, *448*, 571–574.
4. Bunch, J. S.; Verbridge, S. S.; Alden, J. S.; van der Zande, A. M.; Parpia, J. M.; Craighead, H. G.; McEuen, P. L. Impermeable Atomic Membranes from Graphene Sheets. *Nano Lett.* **2008**, *8*, 2458–2462.
5. Stoller, M. D.; Park, S. J.; Zhu, Y. W.; An, J. H.; Ruoff, R. S. Graphene-Based Ultracapacitors. *Nano Lett.* **2008**, *8*, 3498–3502.
6. Park, S.; Ruoff, R. S. Chemical Methods for the Production of Graphenes. *Nat. Nanotechnol.* **2009**, *4*, 217–224.
7. Eda, G.; Lin, Y. Y.; Miller, S.; Chen, C. W.; Su, W. F.; Chhowalla, M. Transparent and Conducting Electrodes for Organic Electronics from Reduced Graphene Oxide. *Appl. Phys. Lett.* **2008**, *92*, 3.
8. Eda, G.; Fanchini, G.; Chhowalla, M. Large-Area Ultrathin Films of Reduced Graphene Oxide as a Transparent and Flexible Electronic Material. *Nat. Nanotechnol.* **2008**, *3*, 270–274.
9. Stankovich, S.; Dikin, D. A.; Dommett, G. H. B.; Kohlhaas, K. M.; Zimney, E. J.; Stach, E. A.; Piner, R. D.; Nguyen, S. T.; Ruoff, R. S. Graphene-Based Composite Materials. *Nature* **2006**, *442*, 282–286.
10. Ramanathan, T.; Abdala, A. A.; Stankovich, S.; Dikin, D. A.; Herrera-Alonso, M.; Piner, R. D.; Adamson, D. H.; Schniepp, H. C.; Chen, X.; Ruoff, R. S.; Nguyen, S. T.; Aksay, I. A.; Prudhomme, R. K.; Brinson, L. C. Functionalized Graphene Sheets for Polymer Nanocomposites. *Nat. Nanotechnol.* **2008**, *3*, 327–331.
11. Dikin, D. A.; Stankovich, S.; Zimney, E. J.; Piner, R. D.; Dommett, G. H. B.; Evmenenko, G.; Nguyen, S. T.; Ruoff, R. S. Preparation and Characterization of Graphene Oxide Paper. *Nature* **2007**, *448*, 457–460.
12. Park, S.; Lee, K. S.; Bozoklu, G.; Cai, W.; Nguyen, S. T.; Ruoff, R. S. Graphene Oxide Papers Modified by Divalent Ions—Enhancing Mechanical Properties *via* Chemical Cross-Linking. *ACS Nano* **2008**, *2*, 572–578.
13. Chen, H.; Muller, M. B.; Gilmore, K. J.; Wallace, G. G.; Li, D. Mechanically Strong, Electrically Conductive, and Biocompatible Graphene Paper. *Adv. Mater.* **2008**, *20*, 3557–3561.
14. Bunch, J. S.; van der Zande, A. M.; Verbridge, S. S.; Frank, I. W.; Tanenbaum, D. M.; Parpia, J. M.; Craighead, H. G.; McEuen, P. L. Electromechanical Resonators from Graphene Sheets. *Science* **2007**, *315*, 490–493.
15. Stankovich, S.; Piner, R. D.; Chen, X. Q.; Wu, N. Q.; Nguyen, S. T.; Ruoff, R. S. Stable Aqueous Dispersions of Graphitic Nanoplatelets *via* the Reduction of Exfoliated Graphite Oxide in the Presence of Poly(sodium 4-styrenesulfonate). *J. Mater. Chem.* **2006**, *16*, 155–158.
16. Stankovich, S.; Dikin, D. A.; Piner, R. D.; Kohlhaas, K. A.; Kleinhammes, A.; Jia, Y.; Wu, Y.; Nguyen, S. T.; Ruoff, R. S. Synthesis of Graphene-Based Nanosheets *via* Chemical Reduction of Exfoliated Graphite Oxide. *Carbon* **2007**, *45*, 1558–1565.
17. Lerf, A.; Buchsteiner, A.; Pieper, J.; Schottl, S.; Dekany, I.; Szabo, T.; Boehm, H. P. Hydration Behavior and Dynamics of Water Molecules in Graphite Oxide. *J. Phys. Chem. Solids* **2006**, *67*, 1106–1110.
18. Buchsteiner, A.; Lerf, A.; Pieper, J. Water Dynamics in Graphite Oxide Investigated with Neutron Scattering. *J. Phys. Chem. B* **2006**, *110*, 22328–22338.
19. Jung, I.; Dikin, S. D.; Cai, W.; Mielke, S. L.; Ruoff, R. S. Effect of Water Vapor on Electrical Properties of Individual Reduced Graphene Oxide Sheets. *J. Phys. Chem. C* **2008**, *112*, 20264–20268.
20. Lerf, A.; He, H. Y.; Forster, M.; Klinowski, J. Structure of Graphite Oxide Revisited. *J. Phys. Chem. B* **1998**, *102*, 4477–4482.

21. Szabo, T.; Berkesi, O.; Forgo, P.; Josepovits, K.; Sanakis, Y.; Petridis, D.; Dekany, I. Evolution of Surface Functional Groups in a Series of Progressively Oxidized Graphite Oxides. *Chem. Mater.* **2006**, *18*, 2740–2749.
22. Cai, W. W.; Piner, R. D.; Stadermann, F. J.; Park, S.; Shaibat, M. A.; Ishii, Y.; Yang, D. X.; Velamakanni, A.; An, S. J.; Stoller, M.; An, J. H.; Chen, D. M.; Ruoff, R. S. Synthesis and Solid-State NMR Structural Characterization of C-13-Labeled Graphite Oxide. *Science* **2008**, *321*, 1815–1817.
23. Gao, W.; Alemany, L. B.; Ci, L. J.; Ajayan, P. M. New Insights into the Structure and Reduction of Graphite Oxide. *Nat. Chem.* **2009**, *1*, 403–408.
24. van Duin, A. C. T.; Dasgupta, S.; Lorant, F.; Goddard, W. A. ReaxFF: A Reactive Force Field for Hydrocarbons. *J. Phys. Chem. A* **2001**, *105*, 9396–9409.
25. Mkhoyan, K. A.; Contryman, A. W.; Silcox, J.; Stewart, D. A.; Eda, G.; Mattevi, C.; Miller, S.; Chhowalla, M. Atomic and Electronic Structure of Graphene-Oxide. *Nano Lett.* **2009**, *9*, 1058–1063.
26. Plimpton, S. J. Fast Parallel Algorithms for Short-Range Molecular Dynamics. *J. Comput. Phys.* **1995**, *117*, 1–19.
27. Chenoweth, K.; van Duin, A. C. T.; Goddard, W. A. ReaxFF Reactive Force Field for Molecular Dynamics Simulations of Hydrocarbon Oxidation. *J. Phys. Chem. A* **2008**, *112*, 1040–1053.
28. Jeffrey, G. A. *An Introduction to Hydrogen Bonding*; Oxford University Press: New York, 1997.
29. Hoover, W. G. Canonical Dynamics: Equilibrium Phase-Space Distributions. *Phys. Rev. A* **1985**, *31*, 1695.
30. Hoover, W. G. Constant-Pressure Equations of Motion. *Phys. Rev. A* **1986**, *34*, 2499.
31. Pratt, L. R. Fluctuation Method for Calculation of Elastic Constants of Solids. *J. Chem. Phys.* **1987**, *87*, 1245.
32. Meyers, M. T.; Rickman, J. M.; Delph, T. J. The Calculation of Elastic Constants from Displacement Fluctuations. *J. Appl. Phys.* **2005**, *98*, 066106.